Space-frequency model of ultrawide-band interactions in free-electron lasers

Y. Pinhasi,* Yu. Lurie, and A. Yahalom
Department of Electrical and Electronic Engineering—Faculty of Engineering, The College of Judea and Samaria, P.O. Box 3, Ariel 44837, Israel
(Received 4 November 2004; published 31 March 2005)

The principle of operation of intense radiation devices such as microwave tubes, free-electron lasers, and masers, is based on a distributed interaction between an electron beam and electromagnetic radiation. Some of the effects emerging during the interaction involve a continuum of frequencies in their broadband spectrum. We developed a three-dimensional, space-frequency theory for the analysis and simulation of radiation excitation and propagation in electron devices and free-electron lasers operating in an ultrawide range of frequencies. The total electromagnetic field (radiation and space-charge waves) is presented in the frequency domain as an expansion in terms of transverse eigenmodes of the (cold) cavity, in which the field is excited and propagates. The mutual interaction between the electron beam and the electromagnetic field is fully described by coupled equations, expressing the evolution of mode amplitudes and electron beam dynamics. The approach is applied in a numerical particle code WB3D, simulating wideband interactions in free-electron lasers operating in the linear and nonlinear regimes.

DOI: 10.1103/PhysRevE.71.036503 PACS number(s): 41.60.Cr, 52.59.Rz

I. INTRODUCTION

Electron devices such as microwave tubes and free-electron lasers (FELs) utilize distributed interaction between an electron beam and electromagnetic radiation. In free-electron lasers, accelerated electrons are passing through an undulator exciting electromagnetic radiation inside a cavity, as illustrated schematically in Fig. 1. Each of the individual electrons in the beam emits a partially coherent radiation, which is called undulator synchrotron radiation [1]. Random electron distribution in the *e*-beam causes fluctuations in current density, identified as shot noise in the beam current [2–5]. The total field is given by a summation of all the contributions of individual electrons to the radiation, resulting in a spontaneous emission [6–14]. In high-gain FELs, utilizing sufficiently long undulators, the spontaneous emission radiation excited in the first part of the undulator is amplified along the remainder of the interaction region, resulting in synchrotron-amplified spontaneous emission (SASE) [15–20]. It was shown that, when the bunch length is shorter than the cooperation length, but still much longer than the radiation wavelength, bunching develops spontaneously along the interaction region, giving rise to a self-induced superfluorescent radiation [21,22]. When the electron beam is premodulated to a single electron bunch shorter than the oscillation period of the emitted radiation [23–27] or to a periodic prebunched beam [28–31], the wave packets of the undulator synchrotron radiation emitted by each of the electrons in the beam add up in the phase, generating a super-radiant emission [32]. Analytical relations between power spectral densities of spontaneous and super-radiant emissions were developed in Ref. [33]. The spectra of these radiation phenomena contain a continuum of frequencies and may be spread over a wide range of wavelengths.

Many models have been developed to describe the mutual interaction between the gain medium (electron beam) and the excited radiation [34–46]. Previous works on multifrequency FEL models were carried out to investigate longitudinal modes dynamics and competition in FEL oscillators [47], sideband effects in waveguide-based FELs [48], radiation dynamics and frequency tuning in high-power free-electron masers [49], and self-amplification of spontaneous emission in the high-gain regime [50]. Most of these models are based on a solution of Maxwell equations and the Lorenz force equation in the time domain. Contrary to these space-time models, formulation of the electromagnetic excitation equations in the frequency domain inherently takes into account dispersive effects arising from the cavity and the gain medium. Moreover, it facilitates consideration of the statistical features of the electron beam and the excited radiation, necessary for the study of broadband phenomena like spontaneous emission, synchrotron-amplified spontaneous emission (SASE), super-radiance, and noise.

In this paper we develop a space-frequency model, which describes broadband phenomena occurring in electron devices, masers, and FELs and characterized by a continuum of frequencies. The total electromagnetic field is presented in the frequency domain as a summation of transverse eigenmodes of the cavity in which it is excited and propagates. A

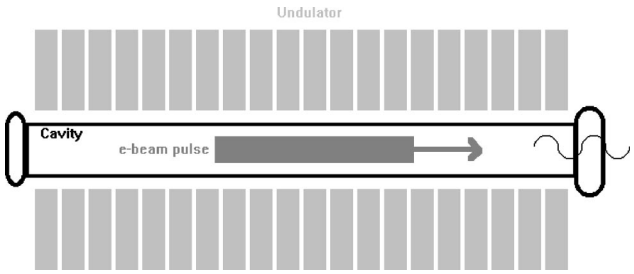

FIG. 1. Schematic illustration of a pulsed beam free-electron laser.

*Electronic address: yosip@eng.tau.ac.il

set of coupled excitation equations, describing the evolution of each transverse mode, is solved self-consistently with beam dynamics equations. This coupled-mode model is employed in a three-dimensional numerical simulation code WB3D [51,52]. The code is used to study the statistical and spectral characteristics of multimode radiation generation in a free-electron laser, operating in various operational parameters. The theory is demonstrated also in the case of "grazing", when the group velocity of the radiation mode is equal to the axial velocity of the electrons, resulting in a wideband interaction between the electron beam and the generated radiation.

II. PRESENTATION OF THE ELECTROMAGNETIC FIELD IN THE FREQUENCY DOMAIN

The electromagnetic field in the time domain is described by the space-time electric $\mathbf{E}(\mathbf{r},t)$ and magnetic $\mathbf{H}(\mathbf{r},t)$ signal vectors. Here, $\mathbf{r}$ stands for the (x,y,z) coordinates, where (x,y) are the transverse coordinates and z is the axis of propagation. The Fourier transform of the electric field is defined by

$$\mathbf{E}(\mathbf{r},f)=\int_{-\infty}^{+\infty}\mathbf{E}(\mathbf{r},t)e^{+j2\pi ft}\,dt, \tag{1}$$

where f denotes the frequency. A similar expression is defined for the Fourier transform $\mathbf{H}(\mathbf{r},f)$ of the magnetic field. Since the electromagnetic signal is real [i.e., $\mathbf{E}^*(\mathbf{r},t)=\mathbf{E}(\mathbf{r},t)$], its Fourier transform satisfies $\mathbf{E}^*(\mathbf{r},f)=\mathbf{E}(\mathbf{r},-f)$.

Analytic representation of the signal is given by the complex expression [52]

$$\tilde{\mathbf{E}}(\mathbf{r},t)\equiv\mathbf{E}(\mathbf{r},t)-j\widehat{\mathbf{E}(\mathbf{r},t)}, \tag{2}$$

where

$$\widehat{\mathbf{E}(\mathbf{r},t)}=\int_{-\infty}^{+\infty}\frac{\mathbf{E}(\mathbf{r},t')}{t-t'}dt', \tag{3}$$

is the Hilbert transform of $\mathbf{E}(\mathbf{r},t)$. Fourier transformation of the analytic representation (2) results in a "phasorlike" function $\tilde{\mathbf{E}}(\mathbf{r},f)$ defined in the positive frequency domain and related to the Fourier transform by

$$\tilde{\mathbf{E}}(\mathbf{r},f)=2\mathbf{E}(\mathbf{r},f)u(f)=\begin{cases}2\mathbf{E}(\mathbf{r},f) & f>0\\ 0 & f<0\end{cases}. \tag{4}$$

The Fourier transform can be decomposed in terms of the phasorlike functions according to

$$\mathbf{E}(\mathbf{r},f)=\frac{1}{2}\tilde{\mathbf{E}}(\mathbf{r},f)+\frac{1}{2}\tilde{\mathbf{E}}^*(\mathbf{r},-f), \tag{5}$$

and the inverse Fourier transform is then

$$\mathbf{E}(\mathbf{r},t)=\int_{-\infty}^{+\infty}\mathbf{E}(\mathbf{r},f)e^{-j2\pi ft}\,df=\mathrm{Re}\left\{\int_{0}^{\infty}\tilde{\mathbf{E}}(\mathbf{r},f)e^{-j2\pi ft}\,df\right\}. \tag{6}$$

III. THE WIENER-KHINCHINE AND PARSEVAL THEOREMS FOR ELECTROMAGNETIC FIELDS

The cross-correlation function of the time dependent electric $\mathbf{E}(\mathbf{r},t)$ and magnetic $\mathbf{H}(\mathbf{r},t)$ fields is given by

$$R_{EH}(z,\tau)=\int_{-\infty}^{+\infty}\left\{\int\int[\mathbf{E}(\mathbf{r},t+\tau)\times\mathbf{H}(\mathbf{r},t)]\cdot\hat{\mathbf{z}}\,dx\,dy\right\}dt. \tag{7}$$

Note that for finite energy signals, the total energy carried by the electromagnetic field is given by $\mathcal{W}(z)=R_{EH}(z,0)$.

According to the Wiener-Khinchine theorem, the spectral density function of the electromagnetic signal energy $S_{EH}(z,f)$ is related to the Fourier transform of the cross-correlation function $R_{EH}(z,\tau)$ through the Fourier transformation

$$\begin{aligned}S_{EH}(z,f)&=\int_{-\infty}^{+\infty}R_{EH}(z,\tau)e^{+j2\pi f\tau}\,d\tau\\&=\int\int[\mathbf{E}(\mathbf{r},f)\times\mathbf{H}^*(\mathbf{r},f)]\cdot\hat{\mathbf{z}}\,dx\,dy\\&=\begin{cases}\displaystyle\int\int\int\frac{1}{4}[\tilde{\mathbf{E}}(\mathbf{r},f)\times\tilde{\mathbf{H}}^*(\mathbf{r},f)]\cdot\hat{\mathbf{z}}\,dx\,dy & f>0\\ \displaystyle\int\int\int\frac{1}{4}[\tilde{\mathbf{E}}(\mathbf{r},-f)\times\tilde{\mathbf{H}}^*(\mathbf{r},-f)]^*\cdot\hat{\mathbf{z}}\,dx\,dy & f<0.\end{cases}\end{aligned} \tag{8}$$

Note that, being the Fourier transform of a real function $R_{EH}(z,\tau)$, the resulting energy spectrum (8) satisfies $S_{EH}(z,-f)=S_{EH}^*(z,f)$.

Following Parseval theorem, the total energy carried by the electromagnetic field can also be calculated by integrating the spectral density $S_{EH}(z,f)$ over the entire frequency domain

$$\begin{aligned}\mathcal{W}(z)&=\int_{-\infty}^{+\infty}S_{EH}(z,f)df\\&=\int_{0}^{\infty}\left[\int\int\frac{1}{2}\,\mathrm{Re}\{\tilde{\mathbf{E}}(\mathbf{r},f)\times\tilde{\mathbf{H}}^*(\mathbf{r},f)\}\cdot\hat{\mathbf{z}}\,dx\,dy\right]df.\end{aligned} \tag{9}$$

We identify

$$\frac{d\mathcal{W}(z)}{df}=\frac{1}{2}\,\mathrm{Re}\left\{\int\int[\tilde{\mathbf{E}}(\mathbf{r},f)\times\tilde{\mathbf{H}}^*(\mathbf{r},f)]\cdot\hat{\mathbf{z}}\,dx\,dy\right\}, \tag{10}$$

as the spectral energy distribution of the electromagnetic field (over positive frequencies). Note that for non-negative frequencies $f\geqslant 0$

$$\begin{aligned}\frac{d\mathcal{W}(z)}{df}&=S_{EH}(z,f)+S_{EH}(z,-f)\\&=2\int_{-\infty}^{+\infty}R_{EH}(z,\tau)\cos(2\pi f\tau)d\tau.\end{aligned} \tag{11}$$

IV. MODAL PRESENTATION OF ELECTROMAGNETIC FIELD IN THE FREQUENCY DOMAIN

The phasorlike quantities defined in (4) can be expanded in terms of transverse eigenmodes of the medium in which the field is excited and propagates, as done in Refs. [53–55] for steady-state, single frequency fields. The perpendicular components of the electric and magnetic fields are given in any cross section as a linear superposition of a complete set of transverse eigenmodes

$$\tilde{\mathbf{E}}_\perp(\mathbf{r},f) = \sum_q [C_{+q}(z,f)e^{+jk_{zq}z} + C_{-q}(z,f)e^{-jk_{zq}z}]\tilde{\mathcal{E}}_{q\perp}(x,y),$$
$$\tilde{\mathbf{H}}_\perp(\mathbf{r},f) = \sum_q [C_{+q}(z,f)e^{+jk_{zq}z} - C_{-q}(z,f)e^{-jk_{zq}z}]\tilde{\mathcal{H}}_{q\perp}(x,y). \quad (12)$$

$C_{+q}(z,f)$ and $C_{-q}(z,f)$ are scalar amplitudes of the qth forward and backward modes, respectively, with electric field $\tilde{\boldsymbol{\mathcal{E}}}_{q\perp}(x,y)$ and magnetic field $\tilde{\boldsymbol{\mathcal{H}}}_{q\perp}(x,y)$ profiles and axial wave number

$$k_{zq}(f) = \begin{cases} j\sqrt{k_{\perp q}^2 - k^2} & k < k_{\perp q} \quad \text{(cutoff modes)}, \\ \sqrt{k^2 - k_{\perp q}^2} & k > k_{\perp q} \quad \text{(propagating modes)}, \end{cases} \quad (13)$$

where $k=2\pi f/c$ and $c=1/\sqrt{\varepsilon_0\mu_0}$ is the velocity of light.

Expressions for the longitudinal component of the electric and magnetic fields are obtained after substituting the modal representation (12) of the fields into Maxwell's equations, where source of electric current density $\tilde{\mathbf{J}}(\mathbf{r},f)$ is introduced

$$\tilde{E}_z(\mathbf{r},f) = \sum_q [C_{+q}(z,f)e^{+jk_{zq}z} - C_{-q}(z,f)e^{-jk_{zq}z}]\tilde{\mathcal{E}}_{qz}(x,y) + \frac{1}{j2\pi f\epsilon_0}\tilde{J}_z(\mathbf{r},f),$$
$$\tilde{H}_z(\mathbf{r},f) = \sum_q [C_{+q}(z,f)e^{+jk_{zq}z} + C_{-q}(z,f)e^{-jk_{zq}z}]\tilde{\mathcal{H}}_{qz}(x,y). \quad (14)$$

The evolution of the amplitudes of the excited modes is described by a set of coupled first-order differential equations

$$\frac{d}{dz}C_{\pm q}(z,f) = \mp\frac{1}{2\mathcal{N}_q}e^{\mp jk_{zq}z}\int\int\left[\left(\frac{Z_q}{Z_q^*}\right)\tilde{\mathbf{J}}_\perp(\mathbf{r},f) \pm \hat{\mathbf{z}}\tilde{J}_z(\mathbf{r},f)\right]\cdot\tilde{\mathcal{E}}_q^*(x,y)dx\,dy. \quad (15)$$

The normalization of the field amplitudes of each mode is made via each mode's complex Poynting vector power

$$\mathcal{N}_q = \int\int[\tilde{\mathcal{E}}_{q\perp}(x,y)\times\tilde{\mathcal{H}}_{q\perp}^*(x,y)]\cdot\hat{\mathbf{z}}\,dx\,dy, \quad (16)$$

and the mode impedance is given by

$$Z_q = \begin{cases} \sqrt{\dfrac{\mu_0}{\epsilon_0}}\dfrac{k}{k_{zq}} = \dfrac{2\pi f\mu_0}{k_{zq}} & \text{for TE modes}, \\ \sqrt{\dfrac{\mu_0}{\epsilon_0}}\dfrac{k_{zq}}{k} = \dfrac{k_{zq}}{2\pi f\epsilon_0} & \text{for TM modes}. \end{cases} \quad (17)$$

Substituting the expansion (12) in (10) results in an expression for the spectral energy distribution of the electromagnetic field (over positive frequencies) as a sum of energy spectrum of the excited modes

TABLE I. Operational parameters of millimeter and submillimeter wave free-electron maser.

Accelerator	
Electron beam energy:	E_k=1–6 meV
Electron beam current:	I_0=1 A
Electron beam pulse duration:	T=0.1 ps
Wiggler	
Magnetic induction:	B_w=2000 G
Period:	λ_w=5 cm
Number of periods:	N_w=20
Waveguide	
Rectangular waveguide:	15×7.5 mm
Mode	Cutoff frequency
TE_{01}	20.0 GHz
TE_{21}, TM_{21}	28.3 GHz
TE_{41}, TM_{41}	44.7 GHz
TE_{03}	60.0 GHz

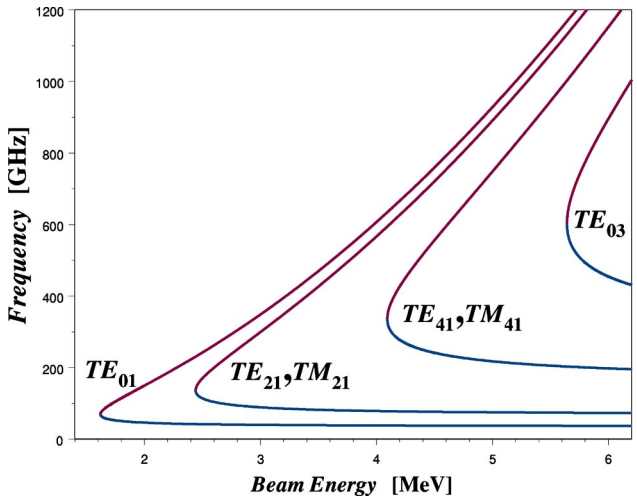

FIG. 2. (Color online) Energy dependence of the dispersion solutions.

TABLE II. Synchronism frequencies for several beam energies.

Beam energy (MeV)	Synchronism frequencies (GHz)			
	TE_{01}	TE_{21}, TM_{21}	TE_{41}, TM_{41}	TE_{03}
1.62	69.6 (grazing)	---	---	---
2.00	46.1, 149.5	---	---	---
2.44	42.0, 230.5	136.2 (grazing)	---	---
3.00	39.8, 348.4	88.9, 299.3	---	---
4.09	38.2, 632.9	78.1, 592.9	336.1 (grazing)	---
5.00	37.5, 927.8	75.0, 890.3	217.5, 747.8	---
5.60	37.3, 1151.0	73.9, 1114.5	203.6, 984.8	602.6 (grazing)

$$\frac{d\mathcal{W}(z)}{df} = \sum_{\substack{q \\ propagating}} \frac{1}{2}[|C_{+q}(z,f)|^2 - |C_{-q}(z,f)|^2]\mathrm{Re}\{\mathcal{N}_q\} + \sum_{\substack{q \\ cutoff}} \mathrm{Im}\{C_{+q}(z,f)C^*_{-q}(z,f)\}\mathrm{Im}\{\mathcal{N}_q\}. \quad (18)$$

V. THE ELECTRON BEAM DYNAMICS

The state of the particle i is described by a six-component vector, which consists of the particle's position coordinates $\mathbf{r}_i=(x_i,y_i,z_i)$ and velocity vector $\mathbf{v}_i$. The velocity of each particle, in the presence of electric $\mathbf{E}(\mathbf{r},t)$ and magnetic $\mathbf{B}(\mathbf{r},t)=\mu_0\mathbf{H}(\mathbf{r},t)$ fields, is found from the Lorentz force equation

$$\frac{d\mathbf{v}_i}{dz} = \frac{1}{\gamma_i}\left\{-\frac{e}{m}\frac{1}{v_{z_i}}[\mathbf{E}(\mathbf{r}_i,t_i)+\mathbf{v}_i\times\mathbf{B}(\mathbf{r}_i,t_i)]-\mathbf{v}_i\frac{d\gamma_i}{dz}\right\}, \quad (19)$$

where e and m are the electron charge and mass, respectively. The fields in Eq. (19) represent the total (dc and ac) forces operating on the particle, and include also the self-field due to space-charge. The Lorentz relativistic factor γ_i of each particle is found from the equation for kinetic energy

$$\frac{d\gamma_i}{dz} = -\frac{e}{mc^2}\frac{1}{v_{z_i}}\mathbf{v}_i\cdot\mathbf{E}(\mathbf{r}_i,t_i). \quad (20)$$

The time it takes a particle to arrive at a position z is a function of the time t_{0i} when the particle entered at $z=0$, and its instantaneous longitudinal velocity $v_{zi}(z)$ along the path of motion

$$t_i(z) = t_{0_i} + \int_0^z \frac{1}{v_{z_i}(z')}dz'. \quad (21)$$

The current distribution is determined by the position and the velocity of the particles in the beam

$$\mathbf{J}(\mathbf{r},t) = -\frac{Q}{N}\sum_{i=1}^{N}\left(\frac{\mathbf{v}_i}{v_{z_i}}\right)\delta(x-x_i)\,\delta(y-y_i)\,\delta[t-t_i(z)]. \quad (22)$$

Here, $Q=I_0T$ is the total charge of the e-beam pulse with dc current I_0 and temporal duration T. The phasorlike current density is given by

$$\tilde{\mathbf{J}}(\mathbf{r},f) = 2u(f)\int_{-\infty}^{+\infty}\mathbf{J}(\mathbf{r},t)e^{+j2\pi ft}dt = -2u(f)\frac{Q}{N}\sum_{i=1}^{N}\left(\frac{\mathbf{v}_i}{v_{z_i}}\right) \times\delta(x-x_i)\,\delta(y-y_i)e^{+j2\pi ft_i(z)}, \quad (23)$$

and its substitution into the excitation equation (15) leads to

$$\frac{d}{dz}C_{\pm q}(z,f) = \pm\frac{1}{\mathcal{N}_q}\frac{Q}{N}\sum_{i=1}^{N}\left\{\frac{1}{v_{z_i}}\left(\frac{Z_q}{Z_q^*}\right)\mathbf{v}_{\perp_p}\cdot\tilde{\mathcal{E}}^*_{\pm q_\perp}(x_i,y_i) + \tilde{\mathcal{E}}^*_{\pm q_z}(x_i,y_i)\right\}e^{j[2\pi ft_i(z)\mp k_{z_q}z]}. \quad (24)$$

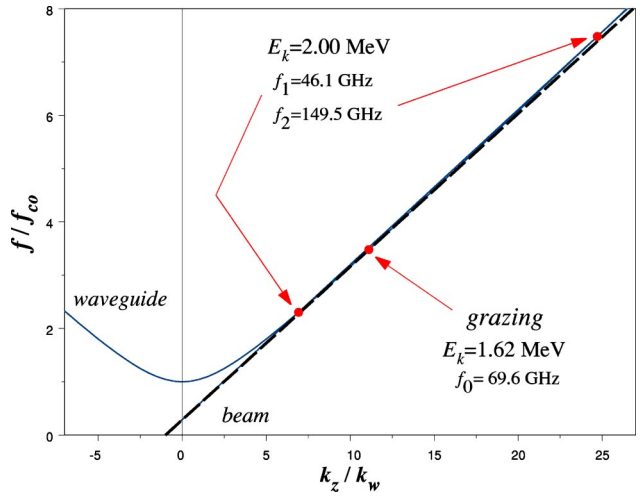

FIG. 3. (Color online) Dispersion solutions for TE_{01} transverse mode for E_k=2 MeV.

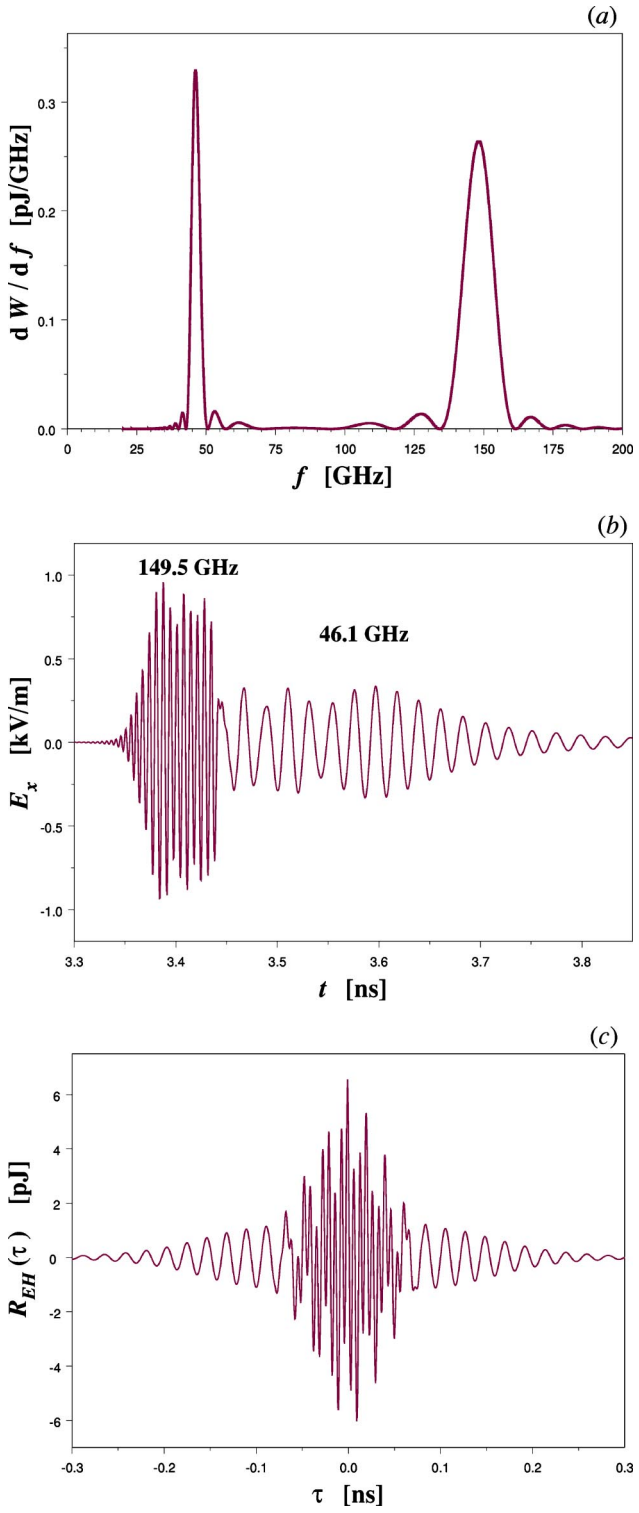

FIG. 4. (Color online) Super-radiant emission from an ultrashort bunch when the beam energy is $E_k = 2$ MeV and a single TE_{01} mode is excited: (a) Energy spectrum; (b) temporal wave packet; and (c) correlation function.

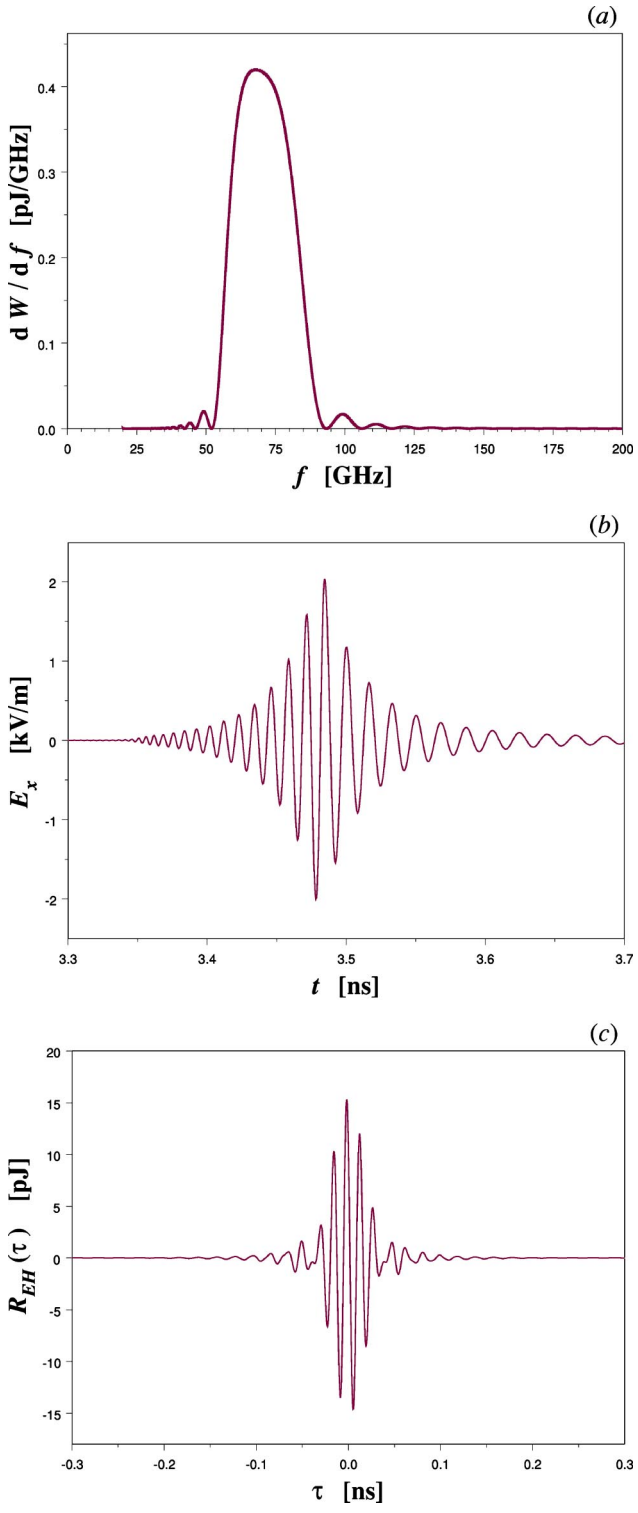

FIG. 5. (Color online) That of Fig. 4, but at grazing condition for mode TE_{01} (the beam energy is $E_k \approx 1.62$ MeV).

The resulting expression, together with the beam dynamics equations (19)–(21), forms a closed set of equations, enabling a self-consistent solution of the electromagnetic fields (radiation and space-charge waves) in electron devices and free-electron lasers. The space-frequency approach described above is employed in the WB3D numerical code, aimed at simulation of free-electron laser operation at wideband frequencies.

Following (20), the total kinetic energy of all particles in the electron beam is given by

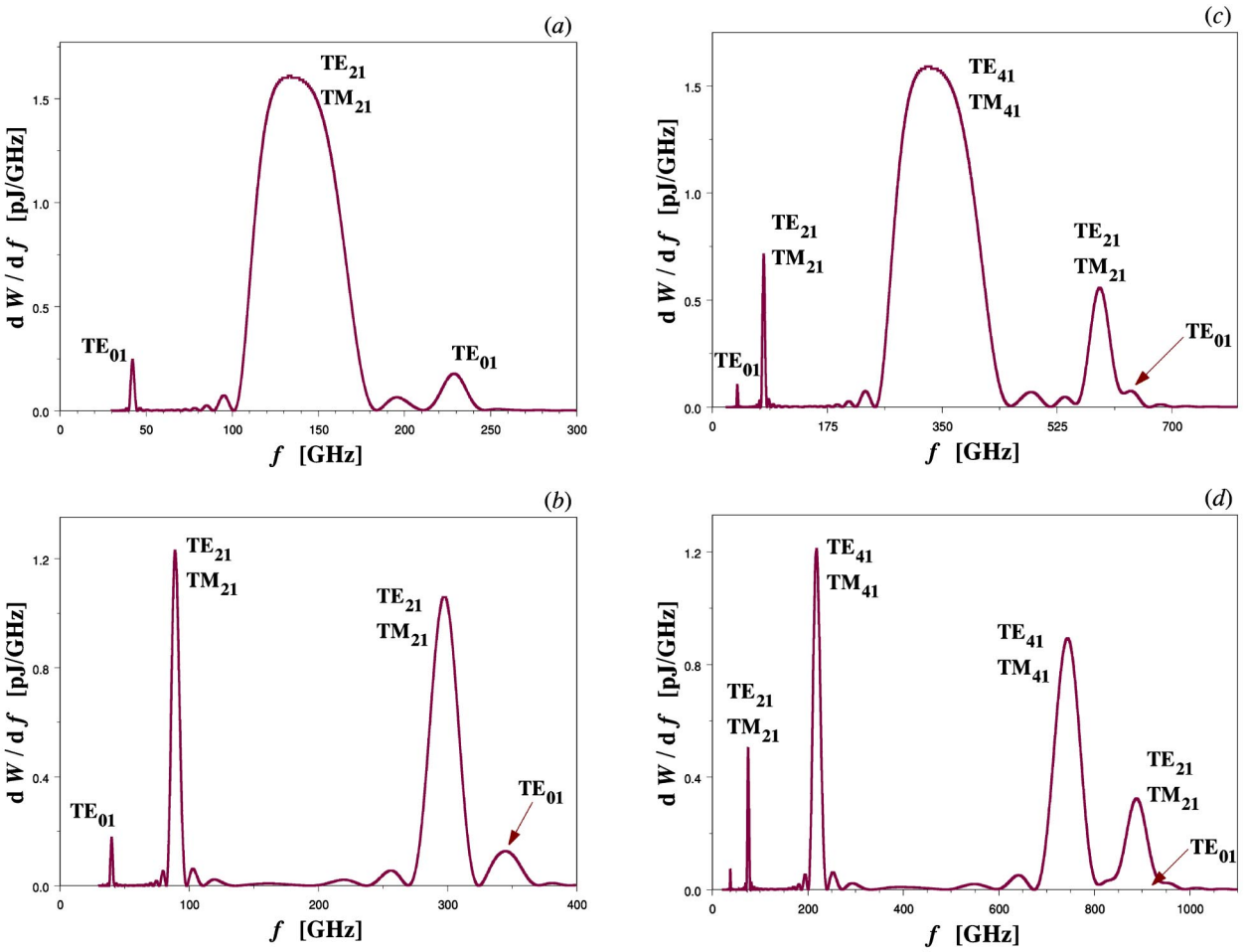

FIG. 6. (Color online) Energy spectra for different acceleration energies: (a) E_k=2.44 MeV (grazing in the TE_{21}, TM_{21} modes); (b) E_k=3.00 MeV; (c) E_k=4.09 MeV (grazing in the TE_{41}, TM_{41} modes); (d) E_k=5.00 MeV.

$$E_{k_{beam}}(z) = \frac{Q}{N}\frac{mc^2}{e}\sum_{i=1}^{N}[\gamma_i(z) - 1]. \tag{25}$$

The change in the kinetic energy of the beam is calculated by substituting Eq. (20) into the derivative of (25)

$$\frac{dE_{k_{beam}}}{dz} = -\frac{Q}{N}\sum_{i=1}^{N}\frac{1}{v_{z_i}}\mathbf{v}_i \cdot \mathbf{E}(\mathbf{r}_i, t_i). \tag{26}$$

Note that the energy conservation

$$\mathcal{W}(z) + E_{k_{beam}}(z) = \mathcal{W}(z=0) + E_{k_{beam}}(z=0), \tag{27}$$

is used in the code for monitoring of numerical calculation accuracy at any plane z along the interaction region.

VI. NUMERICAL RESULTS

To demonstrate the utilization of the model, we present a study of super-radiant emission in a waveguide-based, pulsed beam free-electron maser (FEM), with operational parameters given in Table I. Such a FEM is expected to operate at millimeter and submillimeter (THz) wavelengths. When a FEL utilizes a waveguide, the axial wave number of transverse mode q follows the dispersion relation

$$k_{z_q}(f) = \frac{2\pi}{c}\sqrt{f^2 - f_{co_q}^2}, \tag{28}$$

where $f_{co_q}=(c/2\pi)k_{\perp q}$ is the cutoff frequency of the mode. In synchronism with that mode, the dispersion relation for the electron beam is given by

$$k_{z_q}(f) = \frac{2\pi f}{v_{z0}} + k_w, \tag{29}$$

where v_{z0} is the average velocity of the accelerated electrons and $k_w=2\pi/\lambda_w$ (λ_w is the wiggler's period). The corresponding curves of synchronism frequency vs beam energy for the FEM are shown in Fig. 2. Only waveguide modes which have in their field profile components that interact efficiently with the wiggling electrons are shown. Table II summarizes several examined cases resulting from Eq. (29) in the multi-transverse mode operational regime. For each transverse mode q, the acceleration energy E_k can be set to excite two frequencies corresponding to the "slow" ($v_{g_q}<v_{z0}$) and "fast" ($v_{g_q}>v_{z0}$) synchronism frequencies or to the special case of "grazing," where $v_{g_q}=v_{z0}$ and a single synchronism frequency is obtained. Here

$$v_{g_q} = 2\pi \frac{df}{dk_{z_q}} = \frac{c^2}{2\pi f} k_{z_q}(f), \tag{30}$$

is the group velocity of the excited mode q.

The effect of super-radiance emerges when the duration of the electron beam pulse is much less than the period of the electromagnetic waves expected to be excited at synchronism frequencies according to Table II. The waveguide and e-beam dispersion curves when the acceleration energy is $E_k = 2$ MeV are shown in Fig. 3. In this case a single waveguide mode TE_{01} is excited at two separated synchronism frequencies (slow and fast) 46.1 and 149.5 GHz, respectively. The spectral density of energy flux calculated with the code WB3D is shown in Fig. 4(a). The spectrum peaks at the two synchronism frequencies with mainlobe bandwidth of $\Delta f_{1,2} \approx 1/\tau_{sp_{1,2}}$, where $\tau_{sp_{1,2}} \approx N_w \lambda_w |(1/v_{z_0}) - (1/v_{g_{1,2}})|$ is the slippage time. The corresponding temporal wave packet [shown in Fig. 4(b)] consists of two slow and fast pulses with durations equal to the slippage times modulating carriers at their respective synchronism frequencies. The correlation function given in Eq. (7) is drawn in Fig. 4(c). Lowering the beam energy to $E_k \approx 1.62$ MeV results in grazing between the e-beam and the waveguide dispersion curves at a single synchronism frequency, 69.6 GHz. The spectrum in the case of grazing, the corresponding temporal wave packet, and correlation function are shown in Fig. 5.

As the acceleration energy is increased, transverse modes of higher orders are being excited simultaneously (in addition to the mode TE_{01}), extending the radiation spectrum over a wide range of frequencies from a few tens of GHz to more then THz. Figure 6 shows the energy spectral densities of the excited waveguide modes as the beam energy is increased.

VII. CONCLUSIONS

The presented coupled-mode theory, formulated in the frequency domain, enables development of a three-dimensional model, which can accurately describe wideband interactions between radiation and electron beam in electron devices and free-electron lasers. Space-frequency solution of the electromagnetic equations considers dispersive effects arising from the resonator and gain medium. Such effects play a role also in the special case of grazing, and cannot be accurately treated in approximated space-time approaches. We note that our space-frequency model described here also facilitates the consideration of statistical features of the electron beam and the excited radiation, enabling simulation of the interaction of a free-electron laser operating in the linear and nonlinear regimes.

ACKNOWLEDGMENTS

The research was supported by the Israel Science Foundation and the Israel Ministry of Science.

[1] H. Motz, J. Appl. Phys. **22**, 527 (1951).
[2] W. Schottky, Ann. Phys. **57**, 541 (1918).
[3] S. O. Rice, Bell Syst. Tech. J. **23**, 282 (1944).
[4] S. O. Rice, Bell Syst. Tech. J. **24**, 46 (1945).
[5] L. D. Smulin and H. A. Haus, *Noise in Electron Devices* (The Technology Press of Massachusetts Institute of Technology, Cambridge, MA, 1959).
[6] B. Kincaid, J. Appl. Phys. **48**, 2684 (1977).
[7] J. M. J. Madey, Nuovo Cimento Soc. Ital. Fis., B **50B**, 64 (1979).
[8] A. N. Didenko *et al.*, Sov. Phys. JETP **49**, 973 (1979).
[9] N. M. Kroll, *Physics of Quantum Electronics: Free-electron Generators of Coherent Radiation* (Addison-Wesley, Reading, MA, 1980), Vol. 7.
[10] H. P. Freund *et al.*, Phys. Rev. A **24**, 1965 (1981).
[11] W. B. Colson, IEEE J. Quantum Electron. **QE-17**, 1417 (1981).
[12] H. A. Haus and M. N. Islam, J. Appl. Phys. **54**, 4784 (1983).
[13] K. J. Kim, AIP Conf. Proc. **184**, 565 (1989).
[14] F. V. Hartemann, Phys. Rev. E **61**, 972 (2000).
[15] R. Bonifacio, C. Pellegrini, L. M. Narducei, Opt. Commun. **50**, 373 (1984).
[16] K. J. Kim, Phys. Rev. Lett. **57**, 1871 (1986).
[17] S. Krinsky and L. H. Yu, Phys. Rev. A **35**, 3406 (1987).
[18] R. Bonifacio, L. De Salvo, P. Pierini, N. Piovella, and C. Pellegrini, Phys. Rev. Lett. **73**, 70 (1994).
[19] E. L. Saldin, E. A. Schneidmiller, and M. V. Yurkov, Opt. Commun. **148**, 383 (1998).
[20] J. Andruszkow *et al.*, Phys. Rev. Lett. **85**, 3825 (2000).
[21] R. Bonifacio, C. Maroli, and N. Piovella, Opt. Commun. **68**, 369 (1988).
[22] R. Bonifacio, B. W. J. McNeil, and P. Pierini, Phys. Rev. A **40**, 4467 (1989).
[23] S. Y. Cai, J. Cao, and A. Bhattacharjee, Phys. Rev. A **42**, 4120 (1990).
[24] N. S. Ginzburg and A. S. Sergeev, Opt. Commun. **91**, 140 (1992).
[25] F. Ciocci *et al.*, Phys. Rev. Lett. **70**, 928 (1993).
[26] A. Gover *et al.*, Phys. Rev. Lett. **72**, 1192 (1994).
[27] Y. Pinhasi and A. Gover, Nucl. Instrum. Methods Phys. Res. A **393**, 393 (1997).
[28] M. P. Sirkis and P. D. Coleman, J. Appl. Phys. **28**, 527 (1957).
[29] R. M. Pantell, P. D. Coleman, and R. C. Becker, IRE Trans. Electron Devices **5**, 167 (1958).
[30] I. Schnitzer and A. Gover, Nucl. Instrum. Methods Phys. Res. A **237**, 124 (1985).
[31] A. Doria *et al.*, IEEE J. Quantum Electron. **QE-29**, 1428 (1993).
[32] R. H. Dicke, Phys. Rev. **93**, 99 (1954).
[33] Y. Pinhasi and Yu. Lurie, Phys. Rev. E **65**, 026501 (2002).
[34] W. M. Fawley, D. Prosnitz, and E. T. Scharlemann, Phys. Rev. A **30**, 2472 (1984).
[35] B. D. McVey, Nucl. Instrum. Methods Phys. Res. A **250**, 449 (1986).

[36] A. K. Ganguly and H. P. Freund, Phys. Fluids **31**, 387 (1988).
[37] S. Y. Cai, A. Bhattacharjee, and T. C. Marshall, Nucl. Instrum. Methods Phys. Res. A **272**, 481 (1988).
[38] T. M. Tran and J. S. Wurtele, Comput. Phys. Commun. **54**, 263 (1989).
[39] T.-M. Tran and J. S. Wurtele, Phys. Rep. **195**, XXX(1990).
[40] M. Caplan, Nucl. Instrum. Methods Phys. Res. A **318**, 655 (1992).
[41] M. Caplan *et al.*, Nucl. Instrum. Methods Phys. Res. A **331**, 243 (1993).
[42] Pallavi Jha and J. S. Wurtele, Nucl. Instrum. Methods Phys. Res. A **331**, 243 (1993).
[43] W. M. Fawly, An Informationall Manual for GINGER and its post-processor XPLOTGIN, LBID-2141, CBP Tech Note-104, UC-414, 1995.
[44] H. P. Freund, Phys. Rev. E **52**, 5401 (1995).
[45] S. Reiche, Nucl. Instrum. Methods Phys. Res. A **429**, 429 (1999).
[46] R. J. Dejus, O. Shevchenko, and N. Vinokur, Nucl. Instrum. Methods Phys. Res. A **429**, 225 (1999).
[47] T. M. Antonsen and B. Levush, Phys. Fluids B **1**, 1097 (1989).
[48] E. J. Sternbach, IEEE Trans. Plasma Sci. **18**, 460 (1990).
[49] W. H. Urbanus *et al.*, Phys. Rev. E **59**, 6058 (1999).
[50] N. Piovella, Phys. Plasmas **6**, 3358 (1999).
[51] Y. Pinhasi, Yu. Lurie, and A. Yahalom, Nucl. Instrum. Methods Phys. Res. A **475**, 147 (2001).
[52] Y. Pinhasi, Yu. Lurie, A. Yahalom, and A. Abramovich, Nucl. Instrum. Methods Phys. Res. A **483**, 510 (2002).
[53] N. Markuvitz and J. Schwinger, J. Appl. Phys. **22**, 806 (1951).
[54] L. B. Felsen, *Radiation and Scattering of Waves* (Prentice-Hall, Englewood Cliffs, NJ, 1973).
[55] L. A. Vaynshteyn, *Electromagnetic Waves* (Sovietskoye Radio, Moscow, 1957).